GPS Receiver Satellite/Antenna Selection Algorithm for the Stanford Gravity Probe B Relativity Mission

Jie Li, *Stanford University*
Awele Ndili, *Stanford University*
Lisa Ward, *Ball Aerospace & Technologies Corporation*
Saps Buchman, *Stanford University*

BIOGRAPHY

Jie Li, Ph.D., is a visiting scholar in the Gravity Probe B Relativity Mission at Stanford University. He received his Ph.D. degree from the Chinese Academy of Space Technology in Beijing, P. R. China.

Awele Ndili, Ph.D., is the project manager for GPS receiver development for the Gravity Probe B Relativity Mission at Stanford University. He received his Ph.D. and M.S. degrees from Stanford University. He has been working on GPS systems since 1992.

Lisa Ward, Ph.D., was the former project manager for GPS receiver development for the Gravity Probe B Relativity Mission at Stanford University. She received her Ph.D. degree from University of Colorado.

Saps Buchman, Ph.D., is the payload electronics manager for the Gravity Probe B Relativity Mission at Stanford University. He received his Ph.D. degree in physics from Harvard University.

ABSTRACT

This paper presents a GPS receiver satellite/antenna selection algorithm for the Stanford Gravity Probe B Relativity Mission. A Trimble Advanced Navigation Sensor Vector receiver onboard the space vehicle, a four-antenna six-channel GPS receiver, will provide real-time navigation solutions for orbit trim and raw measurements for ground post-processing, both for more accurate position and velocity and for attitude solutions. The GPS receiver satellite/antenna selection algorithm will determine the visibility of GPS satellites and assign a satellite and a master antenna to each receiver channel in order to maintain signal tracking. In this paper a new four-step GPS satellite selection algorithm is presented, which shows good performance with much less computations compared to the conventional algorithms. The smooth transfer between subsequent GPS satellite sets is also considered in the algorithm, such that continuity of the navigation data is maintained. The antenna selection algorithm is designed to maximize the signal to noise ratio of each master antenna. This paper also presents simulation results of performance comparisons of this new algorithm with conventional algorithms.

INTRODUCTION

The Stanford Gravity Probe B Relativity Mission is a space experiment designed to test Einstein's theory of General Relativity [1]. The Gravity Probe B space vehicle (GP-B) will operate in a polar, circular orbit at the altitude of 650 km, and will roll in the direction of a guide star with a period ranging from 1 minute to 3 minutes. A Trimble Advanced Navigation Sensor (TANS) Vector receiver onboard GP-B, a four-antenna six-channel GPS receiver developed by Trimble Navigation Ltd., will provide real-time navigation solutions for orbit trim and raw measurements for ground post-processing, both for more accurate position and velocity and for attitude solutions.

Previous papers [2] and [3] presented the design of the GPS receiver for the Stanford Gravity Probe B Relativity Mission and the prototypical development efforts including verification test plan and its preliminary results. Compared to the work described in [2] and [3], there are two major changes: (1) The Trimble TANS Vector receiver is used instead of the Loral Tensor receiver; (2) GPS attitude solutions will not be used onboard GP-B, but used for cross-checking on the ground.

With its four antennas, the TANS Vector receiver can track up to six GPS satellites, one on each channel. The RF-signals from four antennas are time-multiplexed, and

a switch sequentially feeds the output signal of each antenna into all six channels. One antenna is assigned as the master antenna for each channel, which provides the signal used for code and carrier tracking, while the other three antennas provide differential phase measurements, referenced to the master antenna. The designation of master antenna can vary from channel to channel, and it can also vary from time to time for each channel.

Fig.1 illustrates the GP-B space vehicle and the GPS antenna configuration. GP-B has a science telescope pointed at an inertially fixed guide star and rolls about its pointing axis at the rate of 0.33~1 rpm. The four antennas are aligned in different directions, such that continuous visibility of GPS satellites will be maintained while GP-B rolls. The forward antennas 1 and 2 are 45^o apart from the bore-sight axis of the telescope, and the aft antennas 3 and 4 are 135^o apart from it. Antennas 1 and 2 are perpendicular to one another and out of phase by 180^o, and so are antennas 3 and 4. The aft set is out of phase by 90^o from the forward set. GPS receivers have never been flown in this configuration before, and it presents a challenge to the software design.

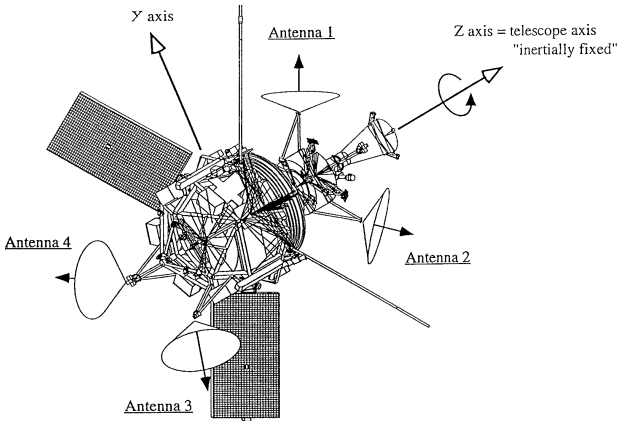

Fig.1 GP-B space vehicle and GPS antenna configuration

The GPS receiver satellite/antenna selection algorithm will determine the visibility of GPS satellites and assign a satellite and a master antenna to each receiver channel in order to maintain signal tracking. The general purpose of the GPS satellite selection algorithm is to minimize the Geometric Dilution Of Precision(GDOP) to improve the position accuracy. However, minimum GDOP algorithms tend to be computationally intensive, while some computationally simpler algorithms have poor GDOP performance. In this paper a new GPS satellite selection algorithm is presented, which shows good performance with much less computations compared to conventional algorithms. The smooth transfer between subsequent GPS satellite sets is also considered in the algorithm, such that continuity of the navigation data is maintained. The antenna selection algorithm is designed to maximize the Signal-to-Noise-Ratio (SNR) of the master antenna.

This paper is organized as follows: First, several coordinate systems are defined. Then the field-of-view (FOV) of antennas is analyzed. The GPS satellite and the antenna selection algorithm are presented separately, and some simulation results are given to compare the performance of this new algorithm with conventional algorithms. Finally, conclusions are derived.

COORDINATE SYSTEMS

As illustrated in Fig.2, several coordinate systems are defined.

Earth-centered inertial coordinate system: O_I is at the center of the Earth, $\vec{Z}_I$ is in the direction of the north pole, $\vec{X}_I$ is perpendicular to $\vec{Z}_I$ and fixed in an inertial direction, and $\vec{Y}_I$ completes the right-handed triad.

Body-centered inertial coordinate system: O_B is at the mass center of GP-B, $\vec{Z}_R$ is in the direction of the guide star, $\vec{X}_R$ lies in the orbital plane of GP-B and makes an acute angle with the direction of the north pole, and $\vec{Y}_R$ completes the right-handed triad.

Body-centered body-fixed coordinate system: O_B is at the mass center of GP-B, $\vec{Z}_B$ is aligned in the bore-sight axis of the science telescope, $\vec{X}_B$ and $\vec{Y}_B$ are fixed to the body of GP-B and complete the right-handed triad.

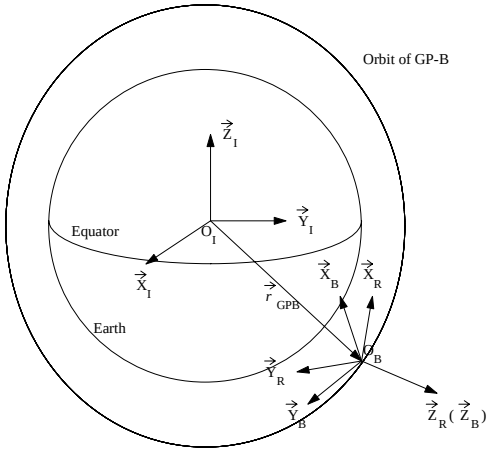

Fig.2 Coordinate systems

FIELD-OF-VIEW OF ANTENNAS

The four antennas are aligned in different directions. The nominal azimuth and elevation angles of the four antennas are given in Table 1, and the components of the pointing axes in $O_B - \vec{X}_B\vec{Y}_B\vec{Z}_B$ are

$$Va_{1-B} = \begin{bmatrix} 0 & \sqrt{2}/2 & \sqrt{2}/2 \end{bmatrix}^T \quad (1)$$

$$Va_{2-B} = \begin{bmatrix} 0 & -\sqrt{2}/2 & \sqrt{2}/2 \end{bmatrix}^T \quad (2)$$

$$Va_{3-B} = \begin{bmatrix} \sqrt{2}/2 & 0 & -\sqrt{2}/2 \end{bmatrix}^T \quad (3)$$

$$Va_{4-B} = \begin{bmatrix} -\sqrt{2}/2 & 0 & -\sqrt{2}/2 \end{bmatrix}^T \quad (4)$$

	Azimuth angle	Elevation angle
Antenna 1	90^o	45^o
Antenna 2	270^o	45^o
Antenna 3	0^o	-45^o
Antenna 4	180^o	-45^o

Table 1. Azimuth and elevation angles of antennas

Fig.3 shows the FOV of four antennas separately in $O_B - \vec{X}_B\vec{Y}_B\vec{Z}_B$. The ellipses are traces with same antenna elevation angles, which are 10^o, 20^o …, 80^o from the outer to inner ellipses. Two factors are considered in the analysis of FOV of GPS antennas: (1) A mask angle is used to specify the antenna elevation angle below which GPS satellites cannot be tracked on the antenna. The nominal value of the mask angle is 10^o. (2) The FOV of the antenna is also obstructed by some structural parts of GP-B, such as the sunshade and solar arrays.

Fig.4 shows the combined FOV of four antennas. The lines denote the edges of the FOV for each antenna. Since the FOVs for the antennas overlap, the numbers in each area denote which antennas share that portion of the view. It is clear that the combined FOV of the four antennas covers the entire sky with a solid angle of 4π steradian. Any GPS satellite visible to GP-B is located in the FOV of at least 1 antenna, and at most 3. So the GPS satellite/antenna selection algorithm can be divided into two independent steps: (1) Select six satellites from all GPS satellites visible to GP-B and assign them to six channels; (2) Assign a master antenna to each channel to maintain visibility of the GPS satellite.

SATELLITE SELECTION ALGORITHM

Geometry of GPS satellites with minimum GDOP

The GDOP describes the general relationship between the errors in the pseudo-range measurements by the GPS receiver to the user position accuracy. In order to improve the GPS-based positioning accuracy, the GPS satellite selection algorithm should minimize GDOP of the selected GPS satellites.

From the almanacs of GPS satellites, the components of the position vector of a GPS satellite *j* (*j*=1, …, 32) in $O_I - \vec{X}_I\vec{Y}_I\vec{Z}_I$ can be determined, which is denoted as r_{j-I}. Based on orbit parameters of GP-B, the components of its position vector in $O_I - \vec{X}_I\vec{Y}_I\vec{Z}_I$ can also be determined, which is denoted as r_{GPB-I}. So the unit vector pointing from GP-B to the GPS satellite *j* is $e_{j-I} = (r_{j-I} - r_{GPB-I}) \Big/ \left| r_{j-I} - r_{GPB-I} \right|$, where $\left| r_{j-I} - r_{GPB-I} \right|$ is the magnitude of $r_{j-I} - r_{GPB-I}$.

Signals from four GPS satellites are required to determine the 3-dimensional position and the user clock bias. Suppose the four GPS satellites are indexed as *j1, j2, j3, j4*, the GDOP is given as follows:

$$GDOP(j1, j2, j3, j4) = tr[(G^T G)^{-1}] \quad (5)$$

where

$$G = \begin{bmatrix} e_{j1-I,x} & e_{j1-I,y} & e_{j1-I,z} & 1 \\ e_{j2-I,x} & e_{j2-I,y} & e_{j2-I,z} & 1 \\ e_{j3-I,x} & e_{j3-I,y} & e_{j3-I,z} & 1 \\ e_{j4-I,x} & e_{j4-I,y} & e_{j4-I,z} & 1 \end{bmatrix} \quad (6)$$

The geometry of four satellites with minimum GDOP is illustrated in Fig.5, where one satellite A is at the zenith, and the other three satellites B, C and D are all equally spaced at 120^o, and placed 109.47^o apart from A to provide a regular tetrahedron[4, 5]. The minimum GDOP is 1.5811.

Define a coordinate system: O_a is at the position of the user, $\vec{Z}_a$ is in the direction of satellite A, $\vec{X}_a$ is perpendicular to $\vec{Z}_a$ and has satellite B in the plane $O_a - \vec{Z}_a\vec{X}_a$, and $\vec{Y}_a$ completes the right-handed triad. The components of direction vectors of four satellites are

$$V_A = \begin{bmatrix} 0 & 0 & 1 \end{bmatrix}^T \quad (7)$$

$$V_B = \begin{bmatrix} 2\sqrt{2}/3 & 0 & -1/3 \end{bmatrix}^T \quad (8)$$

$$V_C = \begin{bmatrix} -\sqrt{2}/3 & \sqrt{6}/3 & -1/3 \end{bmatrix}^T \quad (9)$$

$$V_D = \begin{bmatrix} -\sqrt{2}/3 & -\sqrt{6}/3 & -1/3 \end{bmatrix}^T \quad (10)$$

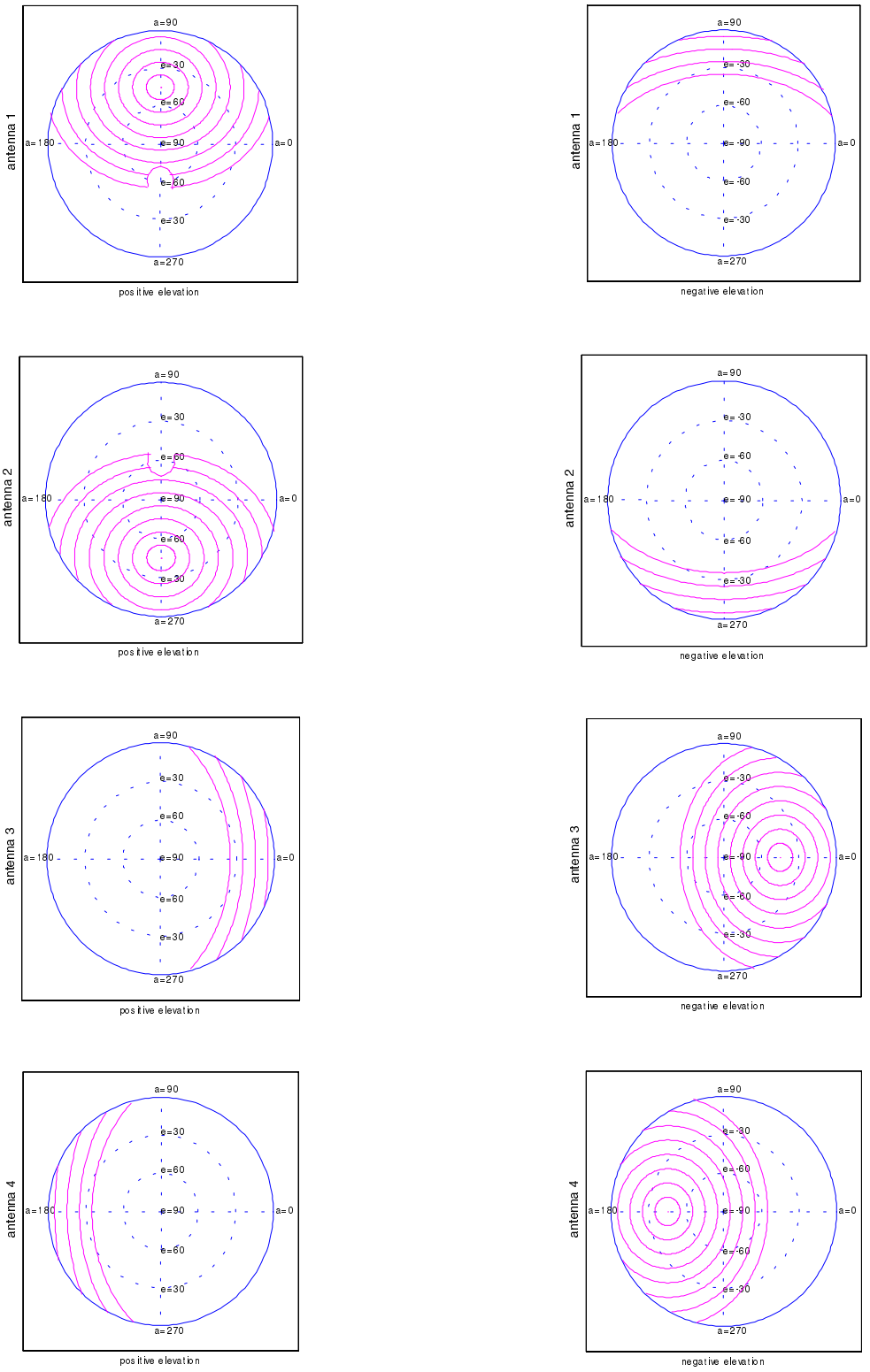

Fig. 3 Field-of-view of antennas

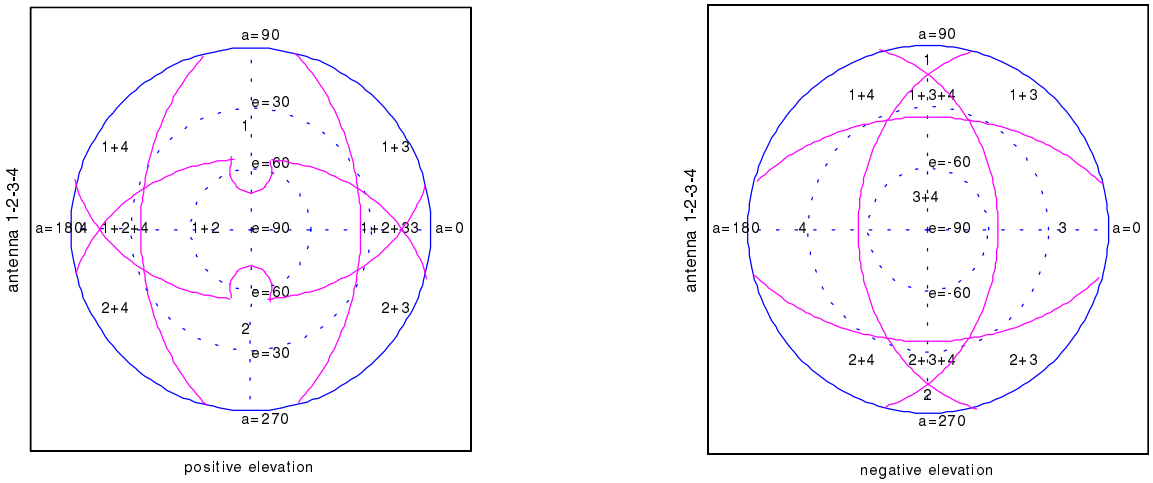

Fig.4 Combined field-of-view of four antennas

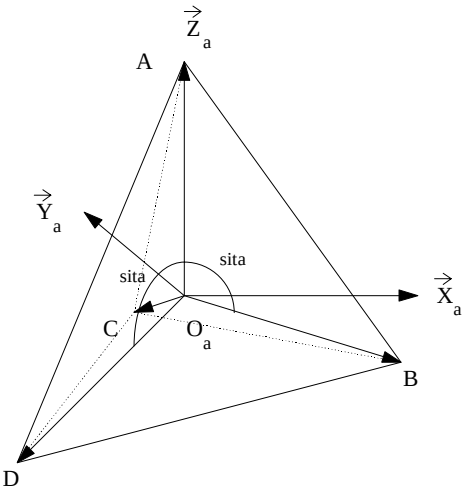

Fig.5 Geometry of GPS satellites with minimum GDOP

Visibility of GPS satellites

The GPS satellites are selected from the satellites visible to GP-B, i.e. the vector pointing from GP-B to the GPS satellite should be above the shell of the Earth occultation.

Let β_j be the angle between the unit vector e_{j-I} and the unit vector of the GP-B position e_{GPB-I}, then the GPS satellite j is visible when the following condition is satisfied

$$\cos(\beta_j) = (e_{j-I})^T e_{GPB-I} > \cos\gamma_{oc} \qquad (11)$$

where γ_{oc} is the threshold angle of the Earth occultation.

Considering the smooth transfer between the subsequent GPS satellite sets (which will be discussed later), it is also required that the selection at time t_n should be made from the satellites which are visible in the time period $\left[t_n - \Delta t_{up},\ \ t_n + \Delta t_{up}\right]$, where Δt_{up} is the update period of the GPS satellite selection algorithm. This gives the GPS receiver time to acquire and track the GPS satellite before using it for the computation of a solution.

Simulations are carried out to study the visibility of GPS satellites with the nominal GP-B orbit parameters and GPS almanacs. Fig.6 illustrates the number of visible GPS satellites in a simulation for a period of 12 hours, where the update period is 1 minute. It is shown that the minimum and maximum number of the visible GPS satellites are 9 and 15 respectively, and the mean number is 11.8.

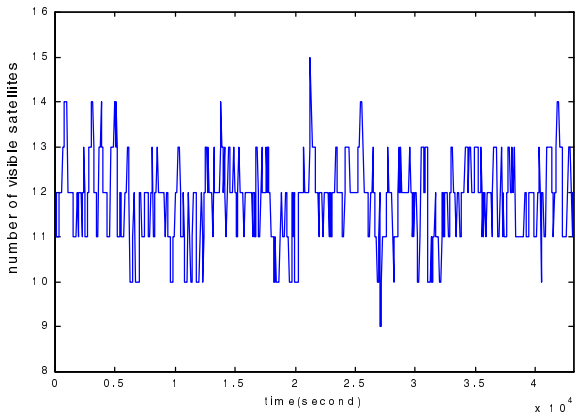

Fig.6 Number of visible GPS satellites

Performance of conventional selection algorithm

Two conventional GPS satellite selection algorithms are discussed as follow.

(a) GDOP is computed for all combinations of four satellites taken from all visible satellites. Then the combination which gives the smallest GDOP is selected.

(b) First, six satellites with the highest elevation angles are selected, then GDOP is computed for all combinations of four satellites from this group of six, and the combination with the smallest GDOP is selected.

Of course the conventional algorithm (a) results in the minimum GDOP, as illustrated in Fig. 7. Therefore this case is used as the reference when comparing the GDOP performance of various selection algorithms. However, the conventional algorithm (a) requires many computations which would be a burden for the GPS receiver. It is an even more serious problem for the GPS receiver onboard space vehicles, since more GPS satellites are visible in space than from land. Considering the minimum number (9) and maximum number (15) of visible GPS satellites illustrated in Fig.6, the number of GDOP computations are 126 and 1365, respectively.

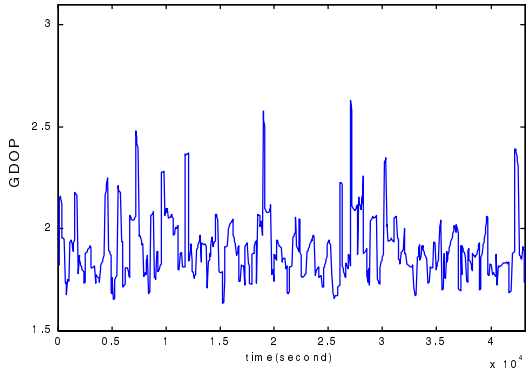

Fig.7 Minimum GDOP of the algorithm (a)

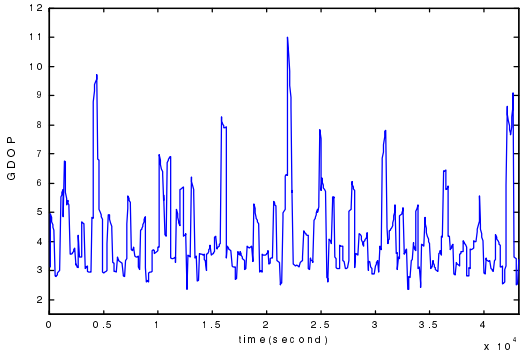

Fig.9 GDOP of the algorithm (b)

Another disadvantage of the conventional algorithm (a) is that the selected satellites may change frequently from one update to the next. If a selected satellite is not one that is currently being tracked, it takes a period of time to acquire and start tracking the newly selected satellite. A maximum of six satellites can be tracked simultaneously, providing two spare satellites. If one or two of the selected satellites are not being tracked, the spare satellites can be used to form a solution until the new satellites are tracked. However, if three or all four satellites selected are not being tracked, this can lead to a loss of navigation data until at least four satellites can be tracked. Fig.8 illustrates the number of changed satellites between subsequent satellite sets selected by the algorithm (a).

The conventional algorithm (b) has much less computations, where the number of GDOP computations is fixed at 15, and it also shows better continuity performance. However, the GDOP of the algorithm at some points is too large to be acceptable. Figs. 9 and 10 show the GDOP and the number of changed GPS satellites between subsequent satellite sets of the conventional algorithm (b) in the simulation.

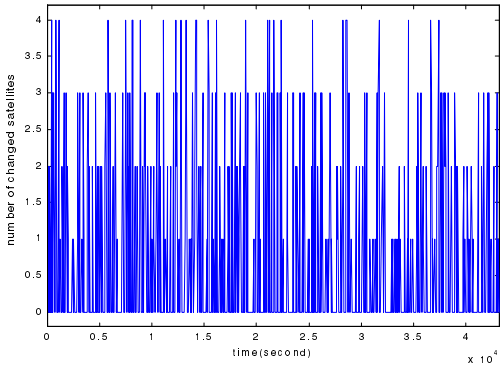

Fig.8 Number of changed satellites of the algorithm (a)

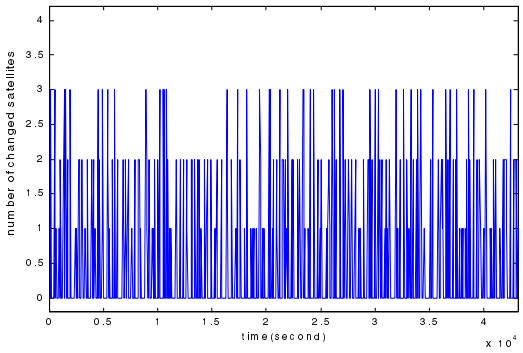

Fig.10 Number of changed satellites of the algorithm (b)

A four-step GPS satellite selection algorithm

This section describes an improved algorithm that has been developed which reduces the number of computations while keeping the GDOP low. Given the components of unit vectors pointing from GP-B to the GPS satellites in the coordinate system $O_I - \vec{X}_I\vec{Y}_I\vec{Z}_I$: e_{1-I}, … , e_{v-I}, (where v is the number of visible GPS satellites), the four GPS satellites can be selected in the following four steps.

Step1: From all visible satellites select Satellite #1, S1, with the highest elevation angle, or

$$(e_{S1-I})^T e_{GPB-I} = \max_j[(e_{j-I})^T e_{GPB-I}] \quad (12)$$
$$j = 1, ..., v$$

Step 2: From the remaining visible satellites select S2 with the largest angular distance to S1, or

$$(e_{S2-I})^T e_{S1-I} = \min_j[(e_{j-I})^T e_{S1-I}] \quad (13)$$
$$j = 1, ..., v \text{ and } j \neq S1$$

Step 3: Based on S1 and S2, a reference triad $\{e_X, e_Y, e_Z\}$ can be established as

$$e_Z = e_{S1-I} \quad (14)$$
$$e_Y = (e_{S1-I} \times e_{S2-I}) \Big/ \left| e_{S1-I} \times e_{S2-I} \right| \quad (15)$$
$$e_X = e_Y \times e_Z \quad (16)$$

A regular tetrahedron $\{R_A, R_B, R_C, R_D\}$ can be defined, whose components of direction vectors of the four vertices in $O_I - \vec{X}_I\vec{Y}_I\vec{Z}_I$ are

$$[V_{RA}\ V_{RB}\ V_{RC}\ V_{RD}] = [e_X\ e_Y\ e_Z] \cdot [V_A\ V_B\ V_C\ V_D] \quad (17)$$

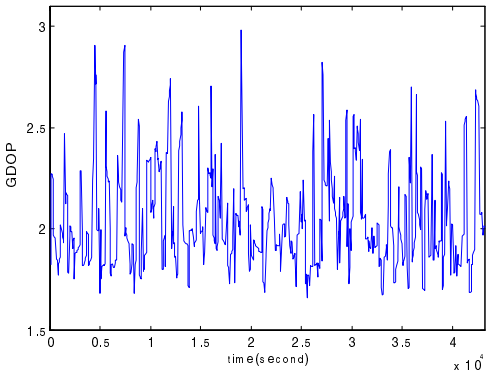

Fig.12 GDOP of the four-step selection algorithm

From the remaining visible satellites S3 is selected which has the smallest angular distance to R_C or R_D, or

$$\max[(e_{S3-I})^T V_{RC}, (e_{S3-I})^T V_{RD}] = \max_j\{\max[(e_{j-I})^T V_{RC}, (e_{j-I})^T V_{RD}]\} \quad (18)$$
$$j = 1, ..., v \text{ and } j \neq S1, S2$$

Step 4: From the remaining visible satellites S4 is selected to minimize GDOP, or

$$GDOP(S1, S2, S3, S4) = \min_j[GDOP(S1, S2, S3, j)] \quad (19)$$
$$j = 1, ..., v \text{ and } j \neq S1, S2, S3$$

Fig.11 illustrates the four-step procedure of the GPS satellite selection. It is clear that the number of the GDOP computations of the algorithm is less than the number of visible satellites. Fig.12 illustrates GDOP of the four-step GPS satellite selection algorithm, and Fig.13 illustrates the number of changed satellites in subsequent satellite sets.

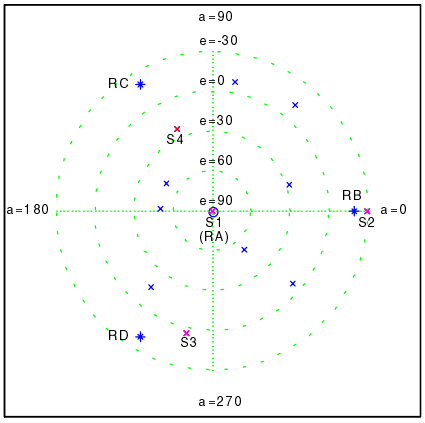

Fig.11 Four-step selection of GPS satellites

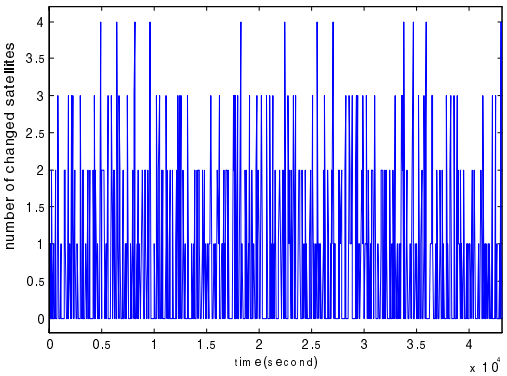

Fig.13 Number of changed satellites of the four-step selection algorithm

GPS satellite selection algorithm with smooth transfer

The selected GPS satellite set is updated periodically. Comparing the subsequent satellite sets, the satellites may be all the same, or one, two, or three satellites may be different. In some cases the four satellites may be totally different. The fewer the number of changed satellites in subsequent sets, the better continuity of the GPS receiver in tracking GPS satellites. In the following discussion an algorithm is presented to make use of the two spare channels for the smooth transfer between subsequent GPS satellite sets so that continuity of navigation data is maintained.

Let the selected set of four satellites at time t_n and t_{n+1} be denoted as

$$G_n = \{S1_n,\ \ S2_n,\ \ S3_n,\ \ S4_n\} \quad (20)$$

$$G_{n+1} = \{S1_{n+1},\ \ S2_{n+1},\ \ S3_{n+1},\ \ S4_{n+1}\} \quad (21)$$

For the smooth transfer from G_n to G_{n+1}, the following 3 cases are considered.

Case 1: Number of changed satellite is 4. An intermediate set $\{S1_{n+1}, S2_{n+1}, B1, B2\}$ is determined, where *B1, B2* are selected from the 4 satellites in G_n to minimize $GDOP\{S1_{n+1}, S2_{n+1}, B1, B2\}$. In this case 6 additional GDOP computations are required. The switch from G_n to G_{n+1} is done as follows: At time t_n four channels are assigned to the four satellites of G_n, and the fifth and sixth channels are assigned to $S1_{n+1}$ and $S2_{n+1}$. When $S1_{n+1}$ and $S2_{n+1}$ are being tracked, the working set is switched to the intermediate set, $S3_{n+1}$ and $S4_{n+1}$ are assigned to the two channels which are used to track satellites other than *B1* and *B2* in G_n. When $S3_{n+1}$ and $S4_{n+1}$ are tracked, the working set is switched to G_{n+1}.

Case 2: Number of changed satellites is 3. An intermediate set {*A0, B1, C1, C2*} is also determined in this case, where *A0* is the only common member in G_n and G_{n+1}, *B1* is selected from the remaining 3 satellites in G_n, and *C1, C2* are selected from the remaining 3 satellites in G_{n+1}. *B1, C1, C2* are determined to minimize *GDOP{A0, B1, C1, C2}*. In this case 9 additional GDOP computations are required. The switch from G_n to G_{n+1} can be done with the intermediate set as in Case 1.

Case 3: Number of changed satellites is less than 3. In this case the two spare channels can be used during the switch from G_n to G_{n+1}, and no additional GDOP computations are required.

Fig.14 illustrates GDOP of the four-step GPS satellite selection algorithm with smooth transfer, and Fig.15 illustrates the GDOP increment compared to the algorithm without smooth transfer. It is shown that the increment of GDOP is generally less than 0.4 when the smooth transfer between subsequent satellite sets is considered. As illustrated, GDOP may decrease in some cases, since the switch through the intermediate set increases the update frequency.

Table 2 compares the performance of the four-step GPS satellite selection algorithm with conventional algorithms in simulations, where the update period is 1 minute. It is shown that the new algorithm presented in this paper has good performance with much less computations. Since the cases where 3 or 4 satellites change in subsequent satellite sets are less than 10%, additional computations for smooth transfer are limited.

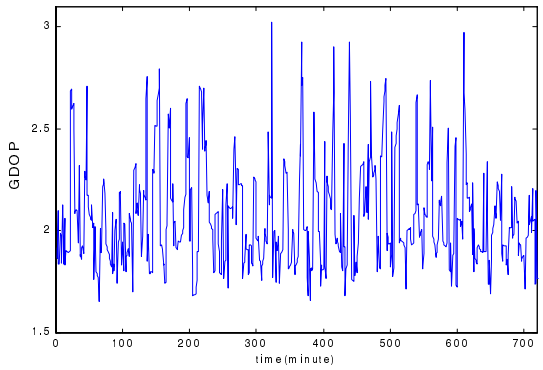

Fig.14 GDOP of the four-step selection algorithm with smooth transfer

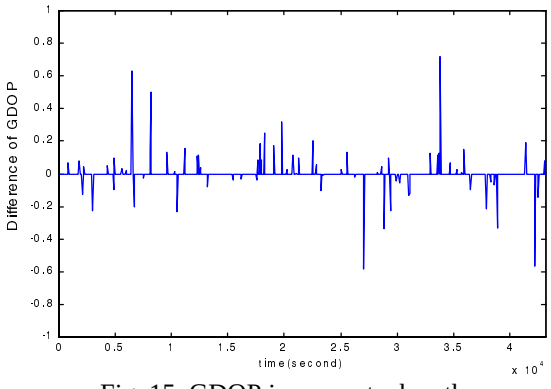

Fig. 15 GDOP increment when the smooth transfer is considered

	GDOP			Statistics in Number of Changed Satellites					Computation
	min	mean	max	4	3	2	1	0	
Conventional Algorithm (a)	1.63	1.90	2.63	30 4.2%	78 10.8%	77 10.7%	68 9.5%	466 64.8%	high
Conventional Algorithm (b)	2.35	4.18	11.03	0 0.0%	47 6.5%	94 13.1%	69 9.6%	509 70.8%	low
Four-Step Selection Algorithm	1.66	2.04	2.98	12 1.7%	59 8.2%	109 15.2%	134 18.6%	405 56.3%	low

Table 2. Comparison of performance of GPS satellite selection algorithms

Performance versus update period

So far we have used a fixed update period of 1 minute. However, 1 minute may be too frequent, and may not permit the receiver to acquire signals on time. Therefore, simulations are carried out to study the performance of the four-step GPS selection algorithm when the update period varies. Figs. 16 and 17 illustrate the number of visible GPS satellites and GDOP of the selection algorithm as a function of update period. It is shown that GDOP doesn't increase very much when the update period is less than 5 minutes. A 5 minute interval results in even lower computation loads.

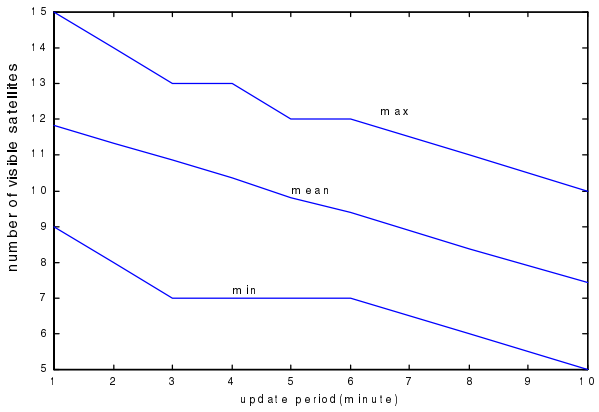

Fig.16 Number of visible satellites versus update period

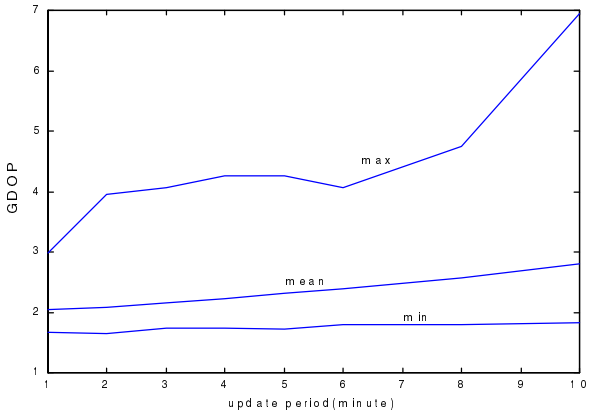

Fig. 17 GDOP versus update period

ANTENNA SELECTION ALGORITHM

While GP-B rolls in the direction of the guide star, the FOV of antennas will also rotate in inertial space. The master antenna has to be transferred among the four antennas to keep tracking a specific GPS satellite. The transfer between two antennas can only be done in the common FOV to prevent tracking discontinuities.

Since the roll period of GP-B is very small compared to the orbit period of GPS satellites, the direction vector of a GPS satellite remains almost fixed in inertial space in a roll period. It traces out a cone in $O_B - \vec{X}_B\vec{Y}_B\vec{Z}_B$, and the body elevation angle (the angle referenced to the plane $O_B - \vec{X}_B\vec{Y}_B$, positive in the direction of $\vec{Z}_B$,) remains constant. Fig.18 shows the areas available for antenna transfer. It is clear that the direction vectors with the body elevation angle of 75^o~90^o remain in the FOV of antennas 1 or 2 during the roll, those with the angle of -90^o~-65^o remain in the FOV of antennas 3 or 4, so no antenna transfer is necessary. The direction vectors with the body elevation angle of 30^o~75^o and -65^o~-30^o must be transferred between antennas 1-2 and 3-4 respectively, while those with the angle of -30^o~30^o must be transferred among antennas 1-2-3, 1-2-4, 1-3-4, or 2-3-4. In Fig.18 the parts of the trace which are available for transfer are plotted in the solid line.

The principle of the antenna selection algorithm is to maximize the SNR of the master antenna, which can be realized in the following two ways:

(1) The receiver has measurements of SNR of four antennas, so the master antenna can be assigned autonomously to the antenna with the largest SNR.

(2) The attitude information from the attitude control subsystem of GP-B is used to determine the direction vector of the GPS satellite in $O_B - \vec{X}_B\vec{Y}_B\vec{Z}_B$, and the master antenna is assigned to the antenna in which the GPS satellite has the highest elevation angle.

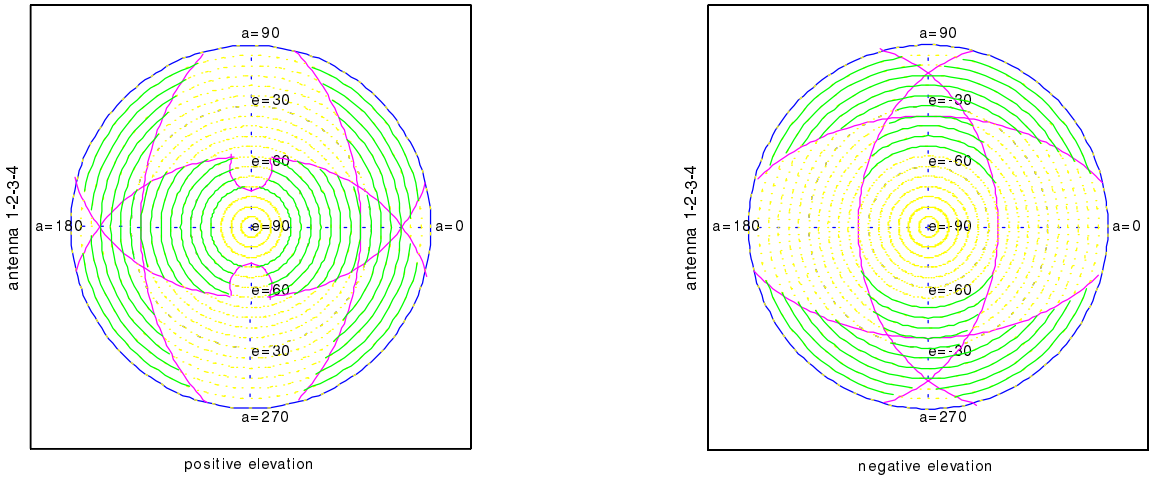

Fig.18 Area available for antenna transfer

Let C_{BI} be the transformation matrix from $O_B - \vec{X}_B\vec{Y}_B\vec{Z}_B$ to $O_I - \vec{X}_I\vec{Y}_I\vec{Z}_I$, the master antenna assigned to track GPS satellite *j* can be determined as

$$(Va_{master-B})^T C_{BI} e_{j-I} = \max_k [(Va_{k-B})^T C_{BI} e_{j-I}] \qquad (22)$$

k=1, 2, 3, 4.

CONCLUSIONS

The GPS receiver satellite/antenna selection algorithm for the Stanford Gravity Probe B Relativity Mission is discussed in this paper, which determines the visibility of GPS satellites and assigns a GPS satellite and a master antenna to each channel of the GPS receiver to maintain signal tracking. The general purpose of the GPS satellite selection algorithm is to minimize GDOP to improve the position accuracy. However, minimum GDOP algorithms tend to be computationally intensive, and some computationally simpler algorithms have poor GDOP performance. In this paper a four-step GPS satellite selection algorithm is presented, which shows good performance with much less computations compared to conventional algorithms. The smooth transfer between subsequent GPS satellite sets is also considered, such that continuity of the navigation data is maintained. The antenna selection algorithm is designed to maximize the SNR of the master antenna. Simulation results demonstrate the good performance of the new algorithm presented in this paper.

ACKNOWLEDGMENTS

Gratitude is acknowledged to NASA for supporting this research under Contract No. NAS8-39225. Trimble Navigation Ltd. is gratefully acknowledged for its support. The authors would also like to thank Lockheed Martin Missiles and Space for their support, especially Jason Suchman for supplying antenna visibility information. Thanks also goes to Dr. Hirohiko Uematsu of NASDA for providing the spacecraft diagram shown in Figure 1.

REFERENCES

1. C.W.F.Everitt, "The Stanford Relativity Gyroscope Experiment(A): History and Overview", in *Near Zero: New Frontiers of Physics*, J.D.Fairbank, J.B.S.Deaver, C.W.F.Everitt, P.F.Michelson, Eds., W.H.Freeman and Company, New York, 1988, pp.587-639.
2. H.Uematsu, B.W.Pakinson and E.G.Lightsey, "GPS Receiver Design and Requirement Analysis for the Stanford Gravity Probe B Relativity Mission", *Proceedings of ION GPS-95*, The Institute of Navigation, Palm Springs, California, Sept. 12-15, 1995, pp.237-246.
3. H.Uematsu and B.W.Parkinson, "GPS Receiver Development and Verification Tests for Stanford Gravity Probe B Relativity Mission: Verification Test Plan and Preliminary Results", *Proceedings of ION GPS-96*, The Institute of Navigation, Kansas City, Missouri, Sept. 17-20, 1996, pp.1377-1385.
4. J.J.Spilker, "Satellite Constellation and Geometric Dilution of Precision", in *Global Positioning System: Theory and Applications, Vol. I*, B.W.Parkinson and J.J.Spilker Eds., AIAA, Inc., 1996, pp.177-208.
5. M.Kihara and T.Okada, "A Satellite Selection Method and Accuracy for the Global Positioning System", *Navigation*, Vol.31, No.1, 1984, pp.8-20.